

# Kinematics of a Gear-Based Spherical Mechanism

Federico Thomas

**Abstract** Kazuki Abe and his collaborators have recently presented an actuated gear-based spherical mechanism called ABENICS. It has received a lot of attention, not only because of its eye-catching motions during operation, but also and mostly, because it can successfully be used when large motion ranges and a high stiffness are required. Nevertheless, the main disadvantage of Abe et al.'s design is that it is an over-actuated mechanism: it requires four instead of only three actuators. In this paper, we propose a variation on this mechanism which requires three actuators, thus simplifying its control and its potential cost. The kinematics of this new mechanism is studied in detail, including its forward and inverse kinematics, as well as its singularities.

## 1 Introduction

Many different parallel spherical mechanisms have been proposed in the past. The mechanism proposed in [3] is probably the most famous one within this category. For more recent alternative designs, see [4] and the references therein. These mechanisms provide high positioning accuracy and excellent dynamic characteristics. Nevertheless, achieving both a large motion range and a high stiffness is a challenging goal for them [2]. A gear-based mechanism might be a good alternative to alleviate these limitations, however it is not obvious how to design a spherical gear to attain arbitrary spherical motions. Although the idea of engraving tooth patterns on a sphere has long been proposed as an improvement for universal joints (see, for example, [5]), it seems that the use of a cross gear engraved over the full surface of a sphere to accomplish general spherical motions has only been recently proposed in [1] under the name of ABENICS. This design consists of a cross spherical gear

---

Federico Thomas  
Institut de Robòtica i Informàtica Industrial (CSIC-UPC), ETSEIB, Diagonal 647, Pavelló E, 08028  
Barcelona, Spain. e-mail: f.thomas@csic.es

**Fig. 1** The cross spherical gear is made by cutting two axisymmetric teeth patterns on a sphere. In this case, the  $x$ - and the  $y$ - axes.

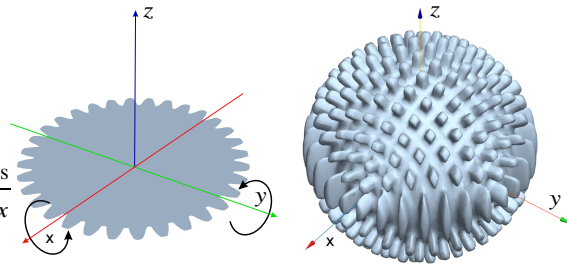
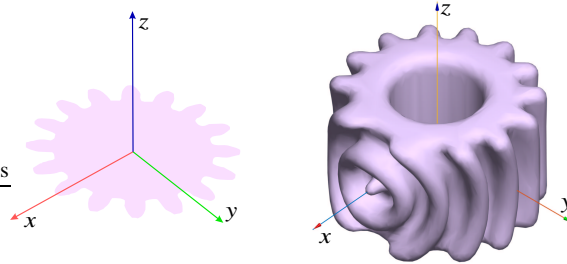


**Fig. 2** The monopoles are made by cutting a teeth pattern on a cylinder that can mesh with the cross spherical gear.



and two monopole gears. The main drawback of the ABENICS design is that it is an over-actuated parallel mechanism: it uses four actuators to control the three degrees of freedom of the moving sphere. The two orientation angles of each monopole are actuated, thus leading to a dependency between them which increases their control complexity. In this paper, we explore the possibility of using three monopoles in such a way that only one orientation angle of each monopole is actuated and the order is left free.

The cross spherical gear is made by cutting two axisymmetric teeth patterns on a sphere. According to Fig. 1, the sphere is first cut around the  $x$ -axis following the profile of an ordinary involute gear, and then this operation is repeated around the  $y$ -axis. The resulting cross spherical gear has four poles located at  $\mathbf{p}_1 = (R, 0, 0)$ ,  $\mathbf{p}_2 = (0, R, 0)$ ,  $\mathbf{p}_3 = (-R, 0, 0)$ , and  $\mathbf{p}_4 = (0, -R, 0)$ .

The monopole gears have a simpler teeth pattern which can mesh with the cross spherical gear. Their radii are half that of the sphere. As shown in Fig. 2, when their  $z$ - and  $x$ - axes are aligned with the rotational axis and the pole, respectively, their cross-sections with the  $xy$ -plane also have the typical involute gear profile. The monopoles have only one pole, and hence their name. In their local reference frames, this pole is located, according to Fig. 2, at  $\mathbf{q} = (R/2, 0, 0)$ .

When meshing a monopole with the spherical gear, we have to previously match its pole with one of the four poles of the sphere. Nevertheless, due to the symmetry of the sphere, observe that it is equivalent to match a monopole with  $\mathbf{p}_1$  or  $\mathbf{p}_2$ , or with  $\mathbf{p}_3$  or  $\mathbf{p}_4$ . Thus, it can simply be said that the monopoles have to be matched with either the  $x$ - or the  $y$ - axis.

The ABENICS mechanism consists of a cross spherical gear and two monopoles located at a right angle on a maximum circle of the sphere. The orientation of each

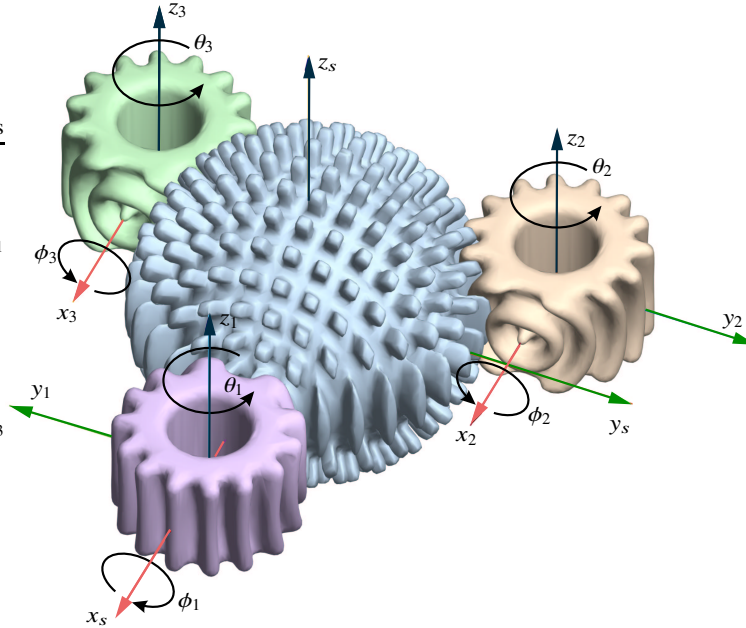


**Fig. 3** Arrangement of a cross spherical gear and three monopoles in the proposed new mechanism. The definition of their local reference frames and associated monopoles orientation angles are also shown. While  $\theta_1$ ,  $\theta_2$ , and  $\theta_3$  are actuated,  $\phi_1$ ,  $\phi_2$ , and  $\phi_3$  are passive.

monopoles is controlled by two actuators. This arrangement of the monopoles, and the fact that their locations are fully controlled, make the kinematics analysis of the mechanism rather trivial. Apparently, there was no simple way to avoid the over-actuation and to keep the kinematics of the mechanism simple at the same time. This is the problem essentially treated in this paper.

This paper is structured as follows. Section 2 presents the proposed variation on the ABENICS mechanism. Section 3 deals with its inverse kinematics. The main challenge imposed by the new design is the resolution of its forward kinematics for which we found a particularly elegant closed-form formula presented in Section 4. The mechanism singularities are deduced in Section 5. The correctness of the presented formulas is verified for an example in Section 6. This paper is concluded in Section 7 with some final considerations.

## 2 The proposed mechanism

In the proposed mechanism, three monopoles are regularly distributed on the  $xy$ -plane of the sphere. According to the reference frames in Fig. 1, Fig. 2, and Fig. 3, their local reference frames in the mechanism will be given by the displacements

$$\mathbf{D}_1 = \mathbf{T}(R + R/2, 0, 0) \mathbf{R}_z(\pi) \mathbf{R}_x(\pi/2), \quad (1)$$

$$\mathbf{D}_2 = \mathbf{R}_z(2\pi/3) \mathbf{D}_1, \quad (2)$$

$$\mathbf{D}_3 = \mathbf{R}_z(-2\pi/3) \mathbf{D}_1. \quad (3)$$

where the term  $\mathbf{R}_x(\pi/2)$  is added to simplify the inverse kinematics as we will show later. The orientation of the sphere will be given by the proper orthogonal matrix  $\mathbf{R} = (r_{ij})_{1 \leq i, j \leq 3}$ .

Without loss of generality, it has been decided to match monopole 1 with the sphere  $x$ -axis, and the other two monopoles with the  $y$ -axis. Matching all the monopoles with the same axis would make any rotation of the sphere about this axis uncontrollable, as it will become clear in the following section. In the proposed design, the angles  $\theta_1$ ,  $\theta_2$ , and  $\theta_3$  around each monopole's  $z$ -axis are actuated, while  $\phi_1$ ,  $\phi_2$ , and  $\phi_3$  are left as passive angles (see Fig. 3).

### 3 Inverse kinematics

Observe that, if a monopole is matched with the sphere  $x$ -axis ( $y$ -axis), its orientation is invariant with respect to any rotation of the sphere about this axis. Indeed, such a rotation induces a lateral sliding of the monopole over the sphere which does not alter its orientation. Thus, only the orientation of the  $x$ -axis ( $y$ -axis) is relevant in the computation of the monopole's orientation.

Since the orientation of the sphere is given by the rotation matrix  $\mathbf{R}$ , we have that the orientation angles of monopole 1 are given by (see Fig. 4)

$$\phi_1 = \text{atan2}(r_{2,1}, r_{3,1}) \quad \text{and} \quad \theta_1 = 2 \arccos(r_{1,1}). \quad (4)$$

In other words, the location of monopole 1 can be expressed in the world reference frame as

$$\mathbf{M}_1 = \mathbf{D}_1 \mathbf{R}_x(\phi_1) \mathbf{R}_z(\theta_1). \quad (5)$$

Now, observe that, due to the invariance of the spherical gear with respect to rotations of  $\pm\pi/2$  about its  $z$ -axis, the orientation angles of monopoles 2 and 3 can still be obtained using (4)—despite they are matched to the sphere  $y$ -axis—by simply performing the substitutions

$$\mathbf{R} \leftarrow \mathbf{R}_z(-2\pi/3) \mathbf{R} \mathbf{R}_z(\pi/2), \quad \text{and} \quad \mathbf{R} \leftarrow \mathbf{R}_z(2\pi/3) \mathbf{R} \mathbf{R}_z(\pi/2), \quad (6)$$

respectively. By performing these substitutions, it can be checked that the orientations of monopoles 2 and 3 are given by the angles

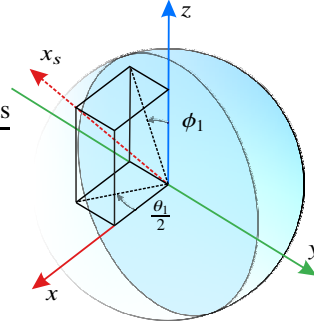


**Fig. 4** Computation of the inverse kinematics for monopole 1 which is matched with the sphere  $x$ -axis, whose orientation is given by  $\mathbf{x}_s = \mathbf{R} \mathbf{x} = (r_{1,1}, r_{2,1}, r_{3,1})^T$ .

$$\begin{aligned}\phi_2 &= \operatorname{atan2}\left(-\frac{1}{2}r_{2,2} - \frac{\sqrt{3}}{2}r_{1,2}, r_{3,2}\right), & \theta_2 &= 2 \arccos\left(\frac{\sqrt{3}}{2}r_{2,2} - \frac{1}{2}r_{1,2}\right), \\ \phi_3 &= \operatorname{atan2}\left(\frac{1}{2}r_{1,2} - \frac{\sqrt{3}}{2}r_{2,2}, r_{3,2}\right), & \theta_3 &= 2 \arccos\left(-\frac{1}{2}r_{1,2} - \frac{\sqrt{3}}{2}r_{2,2}\right).\end{aligned}\quad (7)$$

#### 4 Forward kinematics

The set of equations in (4) and (7) can be rewritten as

$$r_{11} = \cos \frac{\theta_1}{2}, \quad (8)$$

$$r_{21} = k_1 \sin \phi_1, \quad (9)$$

$$r_{31} = k_1 \cos \phi_1, \quad (10)$$

$$r_{12} = \frac{1}{\sqrt{3}}(k_3 \sin \phi_3 - k_2 \sin \phi_4) = -\cos \frac{\theta_2}{2} - \cos \frac{\theta_3}{2}, \quad (11)$$

$$r_{22} = \frac{1}{\sqrt{3}}\left(\cos \frac{\theta_2}{2} - \cos \frac{\theta_3}{2}\right) = -k_2 \sin \phi_2 - k_3 \sin \phi_3, \quad (12)$$

$$r_{32} = k_2 \cos \phi_2 = k_3 \cos \phi_3. \quad (13)$$

where  $k_1$ ,  $k_2$ , and  $k_3$  are constants that cancel when computing the arctangent in the inverse kinematics computations.

Now, observe that using equations (8), (11), and (12), the rotation matrix representing the orientation of the sphere—in terms of the actuated angles,  $\theta_1$ ,  $\theta_2$ , and  $\theta_3$ —can be expressed as

$$\mathbf{R} = \begin{pmatrix} c_1 & -c_2 - c_3 & \boxed{r_{13}} \\ \boxed{r_{21}} & \frac{1}{\sqrt{3}}(c_2 - c_3) & \boxed{r_{23}} \\ \boxed{r_{31}} & \boxed{r_{32}} & \boxed{r_{33}} \end{pmatrix}, \quad (14)$$

where the boxed entries are unknown, and  $c_i = \cos \frac{\theta_i}{2}$ . Thus, the forward kinematics problem reduces to find the different ways in which this matrix can be completed. Since it must be proper orthogonal, the problem can be reduced to solve the system of equations resulting from imposing the algebraic conditions  $\mathbf{R}\mathbf{R}^T = \mathbf{I}$  and  $\det(\mathbf{R})=1$ . Nevertheless, using this approach the problem becomes quite involved. Fortunately, a simpler and neater solution is possible by relying on Euler angles.

An arbitrary rotation matrix can be expressed in terms of XZY Euler angles as

$$\mathbf{R} = \mathbf{R}_x(\alpha_1)\mathbf{R}_z(\alpha_2)\mathbf{R}_y(\alpha_3) = \begin{pmatrix} C_2C_3 & -S_2 & C_2S_3 \\ \boxed{S_1S_3 + C_1C_3S_2} & C_1C_2 & \boxed{C_1S_2S_3 - C_3S_1} \\ \boxed{C_3S_1S_2 - C_1S_3} & C_2S_1 & \boxed{C_1C_3 + S_1S_2S_3} \end{pmatrix}, \quad (15)$$

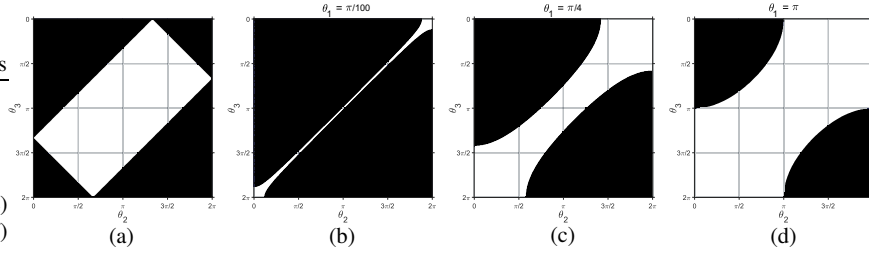


**Fig. 5** The feasible actuation region for  $\theta_2$  and  $\theta_3$  is obtained by intersecting the region in (a) with a region that depends on  $\theta_1$ . This latter region is shown for  $\theta_1 = \pi/100$  (b),  $\theta_1 = \pi/4$  (c), and  $\theta_1 = \pi$  (d). In all cases, the light areas represent the feasible regions.

where  $S_i = \sin \alpha_i$  and  $C_i = \cos \alpha_i$ , and

$$\alpha_1 = \text{atan2}(r_{32}, r_{22}), \quad \alpha_2 = \arcsin(-r_{12}), \quad \text{and} \quad \alpha_3 = \text{atan2}(r_{13}, r_{11}). \quad (16)$$

Since the calculation of  $\alpha_1$ ,  $\alpha_2$ , and  $\alpha_3$  does not require the values of the boxed entries in (15), we can readily conclude from (14) that

$$\begin{aligned} \mathbf{R} = & \mathbf{R}_x \left( \text{atan2} \left( \pm \sqrt{3 - 3(c_2 + c_3)^2 - (c_2 - c_3)^2}, c_2 - c_3 \right) \right) \\ & \mathbf{R}_z (\arcsin(c_2 + c_3)) \\ & \mathbf{R}_y \left( \text{atan2} \left( \pm \sqrt{1 - c_1^2 - (c_2 + c_3)^2}, c_1 \right) \right). \end{aligned} \quad (17)$$

Therefore, given the values of  $\theta_1$ ,  $\theta_2$ , and  $\theta_3$ , four solutions for  $\mathbf{R}$  are obtained, one for each combination of signs of the two square roots appearing in (17).

To finish this section, it is worth remembering that, if  $(\alpha_1, \alpha_2, \alpha_3)$  is a valid set of XYZ Euler angles,  $(\pi + \alpha_1, \pi - \alpha_2, \pi + \alpha_3)$  is as well a valid set. Nevertheless, this fact is irrelevant in our case because both sets lead to the same completion of  $\mathbf{R}$ .

## 5 Singularities

When the pole of monopole  $i = 1, 2, 3$  is in contact with the sphere,  $\phi_i$  is undefined. That is, when the orientation of the sphere is

$$\mathbf{R} = \mathbf{R}_z(n\pi) \mathbf{R}_x(\omega), \quad \mathbf{R} = \mathbf{R}_z\left(\frac{2\pi}{3} + n\pi\right) \mathbf{R}_y(\omega), \quad \text{or} \quad \mathbf{R} = \mathbf{R}_z\left(-\frac{2\pi}{3} + n\pi\right) \mathbf{R}_y(\omega), \quad (18)$$

with  $n \in \mathbb{Z}$  and  $\omega \in \mathbb{R}$ , the mechanism is in a singularity of the inverse kinematics. The set of these singularities can algebraically identified as those cases in which the two arguments of the atan2 functions in (4) or (7) are simultaneously zero.

Besides these rather obvious singularities, we also have the singularities of the forward kinematics. There are values of the actuated angles for which there is a change in the number of forward kinematics solutions. In these cases, at least one of the squared roots arguments in (17) are zero. Moreover, observe that the forward kinematics problem can be solved provided that the following conditions are satisfied

$$(c_2 + c_3)^2 + \frac{1}{3}(c_2 - c_3)^2 \geq 1 \quad \text{and} \quad c_1^2 + (c_2 + c_3)^2 \geq 1. \quad (19)$$

These inequalities define a feasible region in the actuation space whose boundary is the singular set, the set where the number of solutions of the forward kinematics drops from 4 to 2, or 1. While the region defined by the first inequality in (19) is independent of  $\theta_1$  [see Fig. 5 (a)], the second one depends on it [see the resulting region in the  $\theta_1\theta_2$  plane for different values of  $\theta_1$  in Fig. 5 (a), (b), and (c)]. The feasible region obviously results from intersecting both regions.

## 6 Example

Let us consider the particular case in which the actuated angles are arbitrarily chosen as  $\theta_1 = 2.4093$ ,  $\theta_2 = 4.4438$ , and  $\theta_3 = 3.4215$ . Given these values, the forward kinematics of the mechanism can be solved using equation (17). The four obtained results appear in Table 1. To verify the correctness of these results, it is possible to compute the inverse kinematics for each solution using (4) and (7) to recover the value of the actuated angles. Solving the inverse kinematics for each case also gives us the corresponding values of  $\phi_1$ ,  $\phi_2$ , and  $\phi_3$ , that is, the passive joints angles. They are also given in Table 1. The graphical representation of the four assembly modes appears in Fig. 6.

**Table 1** Forward kinematics solutions for  $\theta_1 = 2.4093$ ,  $\theta_2 = 4.4438$ , and  $\theta_3 = 3.4215$ . The corresponding values for the passive joints angles are also included.

Assembly mode	<b>R</b>	$\phi_1$	$\phi_2$	$\phi_3$
1	$\begin{pmatrix} 0.35802 & 0.74558 & 0.56208 \\ 0.93337 & -0.26938 & -0.23719 \\ -0.025432 & 0.60954 & -0.79234 \end{pmatrix}$	1.5981	-0.69768	0.9077
2	$\begin{pmatrix} 0.35802 & 0.74558 & 0.56208 \\ -0.60955 & -0.26938 & 0.74558 \\ 0.7073 & -0.60955 & 0.35802 \end{pmatrix}$	-0.7113	-2.4439	2.2339
3	$\begin{pmatrix} 0.35802 & 0.74558 & -0.56208 \\ -0.60955 & -0.26938 & -0.74558 \\ -0.7073 & 0.60954 & 0.35802 \end{pmatrix}$	-2.4303	-0.69768	0.9077
4	$\begin{pmatrix} 0.35802 & 0.74558 & -0.56208 \\ 0.93337 & -0.26938 & 0.23719 \\ 0.025432 & -0.60954 & -0.79234 \end{pmatrix}$	1.5436	-2.4439	2.2339

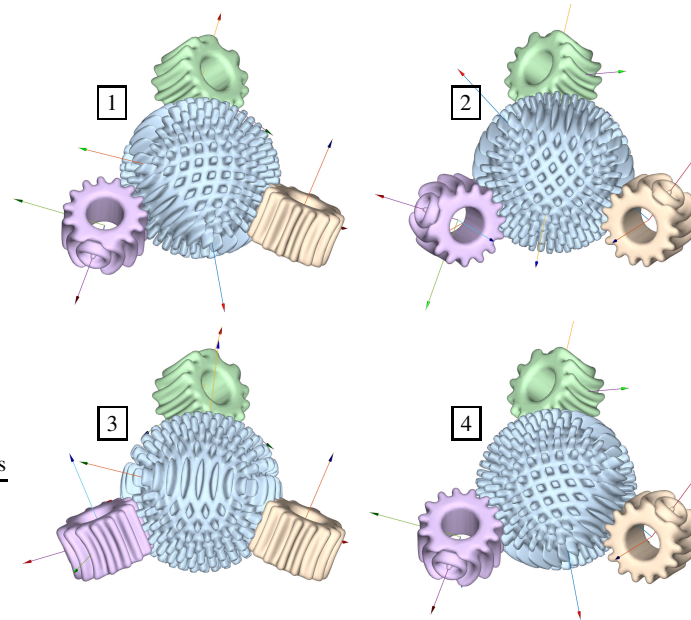


Fig. 6 The four assembly modes given in Table 6.

## 7 Conclusion

We have presented a variation on the recently proposed ABENICS mechanism that simplifies its actuation. The main challenge associated with this variation was the resolution of its forward kinematics and the characterization of its singularities. Curiously enough, however, the use of Euler angles have been shown to be very convenient to complete rotation matrices in a way that allowed us to derive elegant close-form solution formulas for these two problems.

**Acknowledgements** We gratefully acknowledge the financial support of the Spanish Ministry of Economy and Competitiveness through the project PID2020-117509GB-I00.

## References

1. Abe, K., Tadakuma, K., Tadakuma, R.: ABENICS: active ball joint mechanism with three-DoF based on spherical gear meshings, *IEEE Trans. on Robot.*, **37**(5), 1806–1825 (2021)
2. Bajaj, N.M., Spiers, A.J., Dollar, A.M.: State of the art in artificial wrists: A review of prosthetic and robotic wrist design, *IEEE Trans. Robot.*, **35**(1), 261–277 (2019)
3. Gosselin, C.M., St Pierre, E., Gagne, M.: On the development of the agile eye, *IEEE Robot. Automat. Mag.*, **3**(4), 29–37 (1996)
4. Kumar, S., Bongardt, B., Simnofske, M. et al.: Design and kinematic analysis of the novel almost spherical parallel mechanism active ankle, *J. Intell. Robot. Syst.* **94**, 303–325 (2019)
5. Ting, L., Cunyun, P.: On grinding manufacture technique and tooth contact and stress analysis of ring-involute spherical gears, *Mechanism Mach. Theory*, **44**(10), 1807–1825 (2009)